Enhanced optical nonlinearity by photoinduced molecular orientation in absorbing liquids

L. Marrucci, D. Paparo, G. Abbate, and E. Santamato

Istituto Nazionale Fisica della Materia and Università ''Federico II,'' Dipartimento di Scienze Fisiche,
Monte S. Angelo, via Cintia, 80126 Napoli, Italy

M. Kreuzer, P. Lehnert, and T. Vogeler

Institute of Applied Physics, Darmstadt University of Technology, Hochschulstrasse 6, 64289 Darmstadt, Germany

We present a theoretical and experimental study of the molecular orientation induced in a light-absorbing liquid of rodlike molecules by a laser pulse that explains the large enhancement of anisotropic optical Kerr nonlinearity observed in liquids in which a small amount of dye has been dissolved. Our model is based on the assumption that a molecule changes significantly its rotational kinetic and equilibrium behavior when it is electronically excited by the absorption of a photon. The anisotropy of the absorption probability then results in a corresponding orientational anisotropy of the molecules involved in electronic transitions, which in turn orient the whole liquid via intermolecular interactions. To test our model, we performed nanosecond pump-and-probe measurements of nonlinear birefringence at varying pump pulse energy and temperature. In our experiments the host was a liquid-crystal mixture in its isotropic phase and the dye was an anthraquinone derivative. Both the decrease in the nonlinearity enhancement observed for increasing pulse energies and the pretransitional behavior occurring for temperatures approaching the isotropic-nematic transition point are in good agreement with the predictions of our model. The contribution of secondary effects related to light absorption and light-induced heating has been also taken into account in order to properly compare the nonlinearity of an absorbing liquid with that of a transparent one. [S1050-2947(98)03612-9]

PACS number(s): 42.65.An, 34.20.Gj, 42.70.Nq

I. INTRODUCTION

The electric field of a light beam exerts a torque on anisotropic molecules by coupling to the oscillating dipole induced in the molecule by the field itself. The resulting light-induced molecule reorientation is the main mechanism for optical nonlinearity in transparent liquids, the so-called optical Kerr effect [1,2]. In light-absorbing liquids other phenomena, such as thermal lensing and incoherent electronic excitation, may contribute to the material nonlinearity. However, the phenomenon of light-induced molecular orientation itself can be strongly modified when the liquid is absorbing. In particular, as observed recently, mixing small fractions of some dyes in transparent liquids can enhance their nonlinear birefringence resulting from light-induced molecular orientation by orders of magnitude [3,4]. Although still related to molecular reorientation, this effect cannot be explained by a simple enhancement of the optical dipole torque. Its explanation must be sought instead in the transformations occurring in dye molecules as a result of photoinduced electronic excitation and in the consequently altered equilibrium of molecular orientational interactions.

The idea of searching for a dye-induced enhancement of the optical Kerr nonlinearity in liquids came after a similar phenomenon had been observed in the nematic phase of dye-doped liquid crystals [5–7]. For transparent materials, indeed, the driving mechanism of light-induced molecular reorientation of nematic liquid crystals and isotropic liquids is substantially the same. It was then natural to suppose that a similar analogy could be valid also for the still unknown mechanism at work in absorbing materials.

Here we present a study of the molecular orientation induced in an absorbing liquid by a laser light pulse and of the associated optical nonlinearity. Part of our work has already been reported in Ref. [3]. In this paper we describe in detail the theoretical model and its derivation and compare its predictions with our experimental results, taking into proper account secondary effects due to light absorption. In particular, Sec. II is devoted to the theory and is divided into three subsections on the definition of the model and its basic assumptions (Sec. II A), the system dynamical equations in a convenient representation (Sec. II B), the system's steady-state response to a long light pulse (Sec. II C). Section III discusses the experiment and is divided into three subsections on the measurement technique of nonlinear birefringence (Sec. III A), the data corrections for the effects of absorption losses and light-induced heating, necessary for a proper comparison with the case of a transparent material (Sec. III B), and the experimental results (Sec. III C). Finally, a discussion of the results and some conclusive remarks are in Sec. IV.

II. THEORY

A. Model

Let us consider a light-absorbing liquid composed of rodlike molecules in the presence of a linearly polarized optical wave. In our experiments, the material is a mixture of a transparent liquid host and a dye. Therefore, we will refer to this case in presenting the model. However, the same model can be applied also to the case of a pure absorbing material.

We assume that only one excited electronic state of dye molecules is effectively populated by the photoinduced transitions. Therefore, three molecular populations must be con-

sidered, i.e., ground- and excited-state dye molecules and host molecules, which will be denoted by the index $\alpha = g,e,h$, respectively. Let the number of α-type molecules per unit volume and solid angle be $f_\alpha(s_\alpha)$, where s_α is a unit vector specifying the direction of the molecule long axis. Because the system will always exhibit azimuthal symmetry around the optical electric field, f_α will actually depend only on the angle θ between s_α and the field direction. The three functions f_α completely define the state of the system in our model and their dependence on time t defines its dynamics. They can be expanded in a series of Legendre polynomials P_l as

$$f_\alpha(\theta,t) = \frac{1}{4\pi} \sum_{l=0,2,4,\ldots} (2l+1) Q_\alpha^{(l)}(t) P_l(\cos\theta), \quad (1)$$

where

$$Q_\alpha^{(l)}(t) = \int f_\alpha(\theta,t) P_l(\cos\theta) d\Omega \quad (2)$$

are the Legendre moments of the distributions. Because the system also exhibits inversion symmetry, all odd-l moments vanish identically. The infinite set of moments $Q_\alpha^{(l)}(t)$, with even l, therefore provides an equivalent description of the system dynamics. In particular, the zeroth-order moments $Q_\alpha^{(0)} = N_\alpha$ are the total number densities of the populations and the ratios $Q_\alpha^{(2)}/N_\alpha$ are their orientational order parameters. The host density N_h, the total dye density $N_d = N_g + N_e$, and the total density $N_t = N_h + N_d$ are, of course, fixed.

We suppose that the dye electronic transition dipole is parallel to the molecule's geometrical long axis. The light absorption probability per unit time can then be written as

$$p(\theta) = \frac{3\alpha_0}{h\nu N_d} I \cos^2\theta, \quad (3)$$

where I and ν are light intensity and frequency, respectively, α_0 is the absorption coefficient, and h is Planck's constant. The rate of dye electronic transitions from the ground state to the excited state W_e and back W_g is given by

$$W_e(\theta) = -W_g(\theta) = p(\theta) f_g(\theta) - \frac{f_e(\theta)}{\tau_e}, \quad (4)$$

where τ_e is the excited-state lifetime. Note that this expression is based on two important assumptions. One is that stimulated emission is negligible. This is reasonable as, in most dyes, the Stokes shift between absorption and fluorescence spectra makes the excited molecules almost completely off resonance. The other assumption is that the process of vibrational relaxation immediately following each electronic transition (both excitation and decay) has no significant effect on the molecule orientation. For the case of excitation, the success of models of time-resolved fluorescence based on this assumption supports its validity [8]. Moreover, unless the dye molecules are very small, the heat generated by the vibrations is estimated to diffuse away too fast for a large molecular reorientation to occur. In the decay case, however, we must also consider the contribution of

fully nonradiative transitions, which involve a much larger amount of energy converted into heat. This heat could randomize the orientation of those molecules that decay nonradiatively. However, by the time they decay, the orientation of these molecules will already have been largely randomized by rotational Brownian motion occurring in the excited state (as discussed later). Therefore, neglecting this effect will not alter much the model results.

Besides the photoinduced electronic transitions, the molecules are subject to rotational drift and diffusion (i.e., Brownian motion in angle space). In the so-called diffusional approximation, corresponding to the assumption that the reorientation of a molecule occurs in small angular steps, all these processes can be combined in the following set of dynamical rate equations for the angular distributions:

$$\frac{\partial f_\alpha}{\partial t} + \hat{\Lambda}_\alpha f_\alpha = W_\alpha, \quad \alpha = g,e,h. \quad (5)$$

Here $W_h = 0$, as host molecules are not involved in population transitions, and $\hat{\Lambda}_\alpha$ is an operator accounting for the rotational diffusion and drift, defined as

$$\hat{\Lambda}_\alpha = -D_\alpha \frac{1}{\sin\theta} \frac{\partial}{\partial\theta} \sin\theta \left(\frac{\partial}{\partial\theta} + \frac{1}{kT} \frac{\partial U_\alpha}{\partial\theta} \right), \quad (6)$$

where kT is thermal energy, $U_\alpha(\theta)$ is a potential energy controlling the rotational drift and D_α is a rotational diffusion constant. Two contributions to the orientational potential U_α must be considered in our case, i.e.,

$$U_\alpha = U_\alpha^{\mathrm{em}} + U_\alpha^i, \quad (7)$$

accounting for the direct coupling to the external electromagnetic field and for the mean-field effect of intermolecular interactions, respectively. The first term corresponds to the polarization energy

$$U_\alpha^{\mathrm{em}} = -\frac{\eta_\alpha I}{2nc} \cos^2\theta, \quad (8)$$

where $\eta_\alpha/4\pi$ is the anisotropy of molecular optical polarizability, corrected for local-field effects, n is the refractive index, and c is light speed in vacuum. More precisely, we have $\eta_\alpha/4\pi = F^2 \Delta\kappa_\alpha$, where $F = (n^2+2)/3$ is the local-field factor and $\Delta\kappa_\alpha$ is the anisotropy of optical polarizability [2]. The second term U_α^i requires a little more discussion.

A convenient approach is to start from the Gibbs free energy per unit volume G. In a mean-field approximation, G is a functional of the set of distributions f_α. Therefore, we may expand it in a power series and truncate the expansion to the quadratic term, which provides the first nontrivial contribution to G:

$$G \simeq \frac{1}{2N_t} \sum_{\alpha,\beta} \int d\Omega_\alpha \int d\Omega_\beta g(s_\alpha, s_\beta) f_\alpha f_\beta, \quad (9)$$

where $g(s_\alpha, s_\beta)/2N_t$ is the coefficient of the expansion and each integration is over the whole solid angle [9]. Without loss of generality, g can be taken to be symmetric with re-

spect to the exchange of s_α and s_β. The potential U_α^i is then obtained as the functional derivative of G with respect to f_α:

$$U_\alpha^i = \frac{\delta G}{\delta f_\alpha} = \sum_\beta \int d\Omega_\beta g(s_\alpha, s_\beta) f_\beta / N_t. \qquad (10)$$

Next we may expand $g(s_\alpha, s_\beta)$ in a Legendre series in terms of the angle between s_α and s_β. However, here we consider only the contribution of the lowest Legendre term, i.e., we assume

$$g(s_\alpha, s_\beta) = -\frac{1}{2} u_{\alpha\beta} (s_\alpha \cdot s_\beta)^2, \qquad (11)$$

where $u_{\alpha\beta}$ are constants and the isotropic terms are omitted for brevity. Inserting Eq. (11) into Eq. (10) and performing the integration, our final expression for the interaction mean-field potential is obtained:

$$U_\alpha^i(\theta) = -\frac{1}{2} \sum_\beta u_{\alpha\beta} \frac{Q_\beta^{(2)}}{N_t} \cos^2\theta. \qquad (12)$$

The symmetric matrix of energy coefficients $u_{\alpha\beta}$ gauges the orientational intermolecular interactions between pairs of molecules of populations α and β. We note, however, that these coefficients are not strictly molecular quantities. In general, as our derivation shows, they may contain both energy and entropy contributions and may depend on temperature, pressure, and dye concentration, although probably the dependence is weak. Similar considerations apply to the diffusion ''constants'' D_e and D_g.

Equation (5), together with Eqs. (6)–(8), and (12), provides a closed set of integral-differential equations for the system dynamics and completely defines our model. The case of a pure material is obtained by setting $f_h = 0$ in all equations.

B. Dynamical equations for the orientational moments

Using Eqs. (1) and (2), Eq. (5) can be converted into an equivalent set of ordinary differential equations for the moments $Q_\alpha^{(l)}(t)$. Lengthy but straightforward calculations yield

$$\dot{Q}_\alpha^{(l)} + l(l+1)D_\alpha \left\{ Q_\alpha^{(l)} + \left(\frac{\eta_\alpha I}{kTnc} + \sum_\beta \frac{u_{\alpha\beta}Q_\beta^{(2)}}{kTN_t} \right) \left[-\frac{l-1}{(2l-1)(2l+1)} Q_\alpha^{(l-2)} - \frac{1}{(2l-1)(2l+3)} Q_\alpha^{(l)} \right. \right.$$
$$\left. \left. + \frac{l+2}{(2l+1)(2l+3)} Q_\alpha^{(l+2)} \right] \right\} = R_\alpha^{(l)}, \qquad (13)$$

with $R_h^{(l)} = 0$ and

$$R_e^{(l)} = -R_g^{(l)} = -\frac{1}{\tau_e} Q_e^{(l)} + \frac{3\alpha_0 I}{h\nu N_d} \left[\frac{l(l-1)}{(2l-1)(2l+1)} Q_g^{(l-2)} + \frac{2l^2(2l+3)-1}{(2l-1)(2l+1)(2l+3)} Q_g^{(l)} + \frac{(l+1)(l+2)}{(2l+1)(2l+3)} Q_g^{(l+2)} \right]. \qquad (14)$$

These equations can be solved numerically by neglecting all l moments with $l > l_{max}$, where l_{max} must be increased until numerical convergence is achieved. In the following, we will instead adopt an analytical approximate approach that we estimate to be accurate enough for a significant comparison with our experiments. In the dye-doped mixture case, the approximation is based on the following assumptions: (i) light-induced host anisotropy is always very small, i.e., $Q_h^{(l)}/Q_h^{(0)} \ll 1$ for all $l \geq 2$; (ii) the dye moments $Q_\alpha^{(4)}$ are negligible with respect to $Q_\alpha^{(2)}$; and (iii) dye concentration is small, i.e., $N_d/N_t \ll 1$. As we will see, the first two assumptions are automatically verified if the light intensity I is very small, but they may remain valid even at relatively high light intensities. In our experiments we estimate $S_h = Q_h^{(2)}/Q_h^{(0)} < 10^{-3}$ and $Q_e^{(4)}/Q_e^{(2)} \approx Q_g^{(4)}/Q_g^{(2)} \leq 0.2$ at the highest light intensities. Moreover, $N_d/N_t \leq 0.01$. In the case of a pure absorbing liquid, for which $N_d = N_t$, assumption (iii) cannot be made. Therefore, this case needs a separate treatment that remains simple only in the limit of very small light intensity. In this limit, the pure material behaves just as the dye-host mixture, as will be shown.

For brevity, hereafter we use $N_\alpha = Q_\alpha^{(0)}$ and $Q_\alpha = Q_\alpha^{(2)}$. Then Eq. (13) for $l=0$ and $\alpha = e$ is rewritten as

$$\dot{N}_e + \frac{N_e}{\tau_e} = \frac{\alpha_0 I}{h\nu N_d} (N_d - N_e + 2Q_g). \qquad (15)$$

The equations for $l=0$ and $\alpha = g, h$ are unnecessary, as N_h is constant and $N_g(t) = N_d - N_e(t)$. Neglecting Q_g, Eq. (15) is reduced to the standard rate equation for two-level systems. The corresponding characteristic saturation intensity is

$$I_s = \frac{h\nu N_d}{\alpha_0 \tau_e}. \qquad (16)$$

For our case $I_s \sim 10^7$ W/cm^2.

Next let us consider Eq. (13) for $l=2$. For $\alpha = h$, i.e., the host population, the right-hand side vanishes. Moreover, by assumption (i), of the three terms included in the square brackets on the left-hand side only the first is significant. Rearranging the remaining terms, one obtains

$$\dot{Q}_h + 6D_h \left(1 - \frac{u_{hh}N_h}{15kTN_t} \right) Q_h$$
$$= \frac{2D_h N_h}{5kTN_t} \left(\frac{\eta_h N_t I}{nc} + u_{he}Q_e + u_{hg}Q_g \right). \qquad (17)$$

In this equation the second term on the left-hand side is the relaxation term due to rotational diffusion, weakened by the self-interaction energy u_{hh}. At the critical temperature

$$T^* = \frac{u_{hh}N_h}{15kN_t}, \tag{18}$$

the relaxation term vanishes and the isotropic phase is spontaneously unstable. If T^* is above the transition point to the solid phase, then the system will exhibit a nematic liquid-crystalline mesophase below a transition temperature T_c that is slightly higher than T^* [10]. From the relaxation term in Eq. (17), we obtain the relaxation time for the host orientational order, i.e.,

$$\tau_h = \frac{1}{6D_h}\left(\frac{T}{T-T^*}\right). \tag{19}$$

Let us now consider Eq. (13) for $l=2$ and $\alpha=e,g$. On the left-hand side, only the first term of those in curly brackets must be retained, i.e., $Q_\alpha^{(2)}$. This corresponds to considering only light absorption as a driving term for the dye anisotropy, and neglecting the effect of orientational interactions with the host, which is almost isotropic, and with the other dye molecules, which are far from each other. In other words, the latter terms are of the order of S_h or N_d/N_t and are therefore negligible according to assumptions (i) and (iii). Moreover, we may neglect the contribution of $Q_\alpha^{(4)}$ in $R_\alpha^{(2)}$, in accordance with assumption (ii).

The whole model is therefore finally reduced to the set of four differential equations

$$\dot{N}_e + \frac{N_e}{\tau_e} = \frac{\alpha_0 I}{h\nu N_d}(N_d-N_e+2Q_g),$$

$$\dot{Q}_e + \frac{Q_e}{\tau_d} = \frac{2\alpha_0 I}{5h\nu N_d}\left(N_d-N_e+\frac{55}{14}Q_g\right),$$

$$\dot{Q}_g + 6D_g Q_g = -\dot{Q}_e - 6D_e Q_e, \tag{20}$$

$$\dot{Q}_h + \frac{Q_h}{\tau_h} = \frac{6D_h T^*}{Tu_{hh}}\left(\frac{\eta_h N_t}{nc}I + u_{he}Q_e + u_{hg}Q_g\right),$$

where we introduced the overall decay time for the dye moment Q_e,

$$\tau_d = (\tau_e^{-1} + 6D_e)^{-1}. \tag{21}$$

A more formal derivation of these approximate equations can be based on a iterative solution of Eq. (13) for small light intensity I and dye concentration N_d/N_t. However, we point out that Eqs. (20) include terms that are not of the lowest order in the ratio I/I_s in order to describe the effect of absorption saturation (dye bleaching). On the contrary, only terms of the lowest order in N_d/N_t and I/I_K are retained, where $I_K = 15kTnc/\eta_h$ is the intensity for saturation of the ordinary optical Kerr effect due to polarization. This procedure is justified if $I_s \ll I_K$, which is usually the case. In our case $I_K \sim 10^{12}$ W/cm^2, five orders of magnitude larger than I_s. We expect Eqs. (20) to be appropriate for intensities $I \ll I_K$ and $I \leq I_s$. Assumption (ii) that $l>4$ dye moments are

negligible is not justified *a priori* for $I \gg I_s$. However, we performed some numerical calculations including higher l contributions and found that the results changed little, even in this high-intensity range.

Let us now consider the pure liquid case. There is no host, only g and e molecules, and $N_d=N_t=N_h$. For simplicity, we restrict the discussion to the small intensity limit $I \ll I_s$ and $I \ll I_K$ (therefore we give up describing the saturation behavior). After retaining only terms of the lowest order in both I/I_s and I/I_K, we obtain

$$\dot{N}_e + \frac{N_e}{\tau_e} = \frac{\alpha_0 I}{h\nu},$$

$$\dot{Q}_e + \frac{Q_e}{\tau_d} = \frac{2\alpha_0}{5h\nu}I, \tag{22}$$

$$\dot{Q}_g + \frac{Q_g}{\tau_g} = \frac{6D_g T^*}{u_{gg}T}\left(\frac{\eta_g N_t}{nc}I + u_{ge}Q_e\right) - \dot{Q}_e - 6D_e Q_e,$$

where $T^* = u_{gg}/15k$ and $\tau_g = T/6D_g(T-T^*)$.

Before looking for the solutions to Eqs. (20) or (22), let us express the nonlinear birefringence measured by a weak probe light pulse in terms of the dynamical variables of the model. The birefringence is related to the dielectric anisotropy $\Delta\epsilon = \epsilon_\parallel - \epsilon_\perp$, where $\parallel$ and $\perp$ stand for parallel and perpendicular to the pump electric field, respectively. It can be shown that

$$\Delta\epsilon = \sum_\alpha \eta'_\alpha Q_\alpha, \tag{23}$$

where $\eta'_\alpha/4\pi = F'^2 \Delta\kappa'_\alpha$ is the local-field-corrected polarizability anisotropy at the probe wavelength λ'. If $\Delta\epsilon$ is small, the birefringence is given by $\Delta n \simeq \Delta\epsilon/2n$. The ratio $\Delta n/I$ characterizes the anisotropic optical Kerr nonlinearity of the material.

C. Steady-state solution

Here we report and discuss the steady-state solution corresponding to a constant pump light intensity I and to a stationary value of all molecular-distribution moments. This particular solution can be found by solving the algebraic set of equations obtained from Eqs. (20) in the dye-doped case or Eqs. (22) in the pure material case, after setting all time derivatives to zero. In actual experiments the pump light is pulsed and this steady-state solution will represent the asymptotic behavior that is reached by the system after a transient following the beginning of the pulse provided the pulse duration is much longer than the material response τ_h (or τ_g for the pure liquid).

Let us consider first the dye-doped liquid case. The stationary solutions to Eqs. (20) are

$$Q_e = \frac{2\alpha_0 \tau_d}{5h\nu}If(I), \tag{24}$$

$$N_e = \frac{I}{I_s+I}\left(N_d - 2\frac{D_e}{D_g}Q_e\right),$$

$$Q_g = -\frac{D_e}{D_g} Q_e,$$

$$Q_h = \frac{1}{u_{hh}} \frac{T^*}{T-T^*} \left(\frac{\eta_h N_t}{nc} I + \Delta u Q_e \right),$$

where we introduced the molecular parameter

$$\Delta u = u_{he} - \frac{D_e}{D_g} u_{hg} \qquad (25)$$

and the function

$$f(I) = \left[1 + \left(1 + \frac{11 D_e \tau_d}{7 D_g \tau_e} \right) \left(\frac{I}{I_s} \right) + \left(\frac{27 D_e \tau_d}{35 D_g \tau_e} \right) \left(\frac{I}{I_s} \right)^2 \right]^{-1}. \qquad (26)$$

The total dielectric anisotropy is then

$$\Delta \epsilon = \left(\eta_e' - \frac{D_e}{D_g} \eta_g' \right) Q_e + \frac{\eta_h' T^*}{u_{hh}(T-T^*)} \left(\frac{\eta_h N_t}{nc} I + \Delta u Q_e \right). \qquad (27)$$

Let us now discuss the physical meaning of this solution. First, note that light absorption is an anisotropic process and therefore it tends to generate an oriented population of excited dye molecules. At the same time, it leaves an anisotropic hole in the population of ground-state dye molecules. This forcing mechanism is opposed by two relaxation mechanisms: electronic decay, controlled by the lifetime τ_e, and rotational diffusion, controlled by the constants D_e and D_g. The balance between these effects gives rise to the nonzero dye moments Q_e and Q_g. Note, however, that $Q_e + Q_g \neq 0$ only if $D_e \neq D_g$. In other words, the overall dye distribution remains isotropic unless the rotational diffusion has different rates in the excited and ground states. The function $f(I)$ here describes the nonlinear behavior of the dye anisotropy due to saturation of absorption; in particular, $f(I) \simeq 1$, so that $Q_e \propto I$ for $I \ll I_s$, and $f(I) \to 0$, so that $Q_e \to 0$ for $I \to \infty$. Examples of this behavior are plotted in Fig. 1 for several values of the parameter $D_e \tau_d / D_g \tau_e$. Note, in particular, that the dye moment $Q_e \propto I f(I)$ has a maximum at $I = I_{max} = I_s (27 \tau_d D_e / 35 \tau_e D_g)^{-1/2}$. Once the dye populations become anisotropic, they start to act upon the host liquid generating an orienting potential $U_h^i \propto u_{he} Q_e + u_{hg} Q_g = \Delta u Q_e$. Note that a nonzero U_h^i can be ascribed to one or both of the following independent contributions: (i) The overall dye population becomes anisotropic, because $D_e \neq D_g$, and it therefore can orient the host even if $u_{he} = u_{hg}$ and (ii) the overall dye population remains isotropic, because $D_e = D_g$, but its effect on the host is nonetheless anisotropic because the interaction energy in the excited state is different from that in the ground state, i.e., $u_{he} \neq u_{hg}$. The combined effect of these two contributions is expressed by the energy constant Δu. Finally, the molecular potential U_h^i, together with the usual polarization potential U_h^{em} of the optical field, orients the liquid host molecules, i.e., produces a nonzero host order parameter Q_h.

We point out that the anisotropy of dye molecules can be understood as the result of essentially all single-molecule
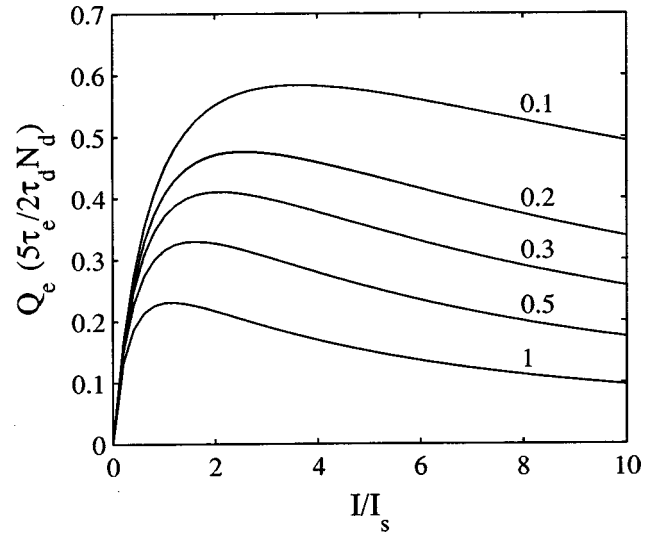

FIG. 1. Theoretical excited-dye distribution moment Q_e, normalized to $2\tau_d N_d / 5\tau_e$, versus light intensity I, normalized to the dye saturation intensity I_s, for several values of the ratio $D_e \tau_d / D_g \tau_e$.

processes, i.e., photon absorption and rotational Brownian motion. On the other hand, the photoinduced orientation of the host is a collective effect driven by dye-host intermolecular interactions and enhanced by host-host interactions.

The dielectric anisotropy (and hence the nonlinear birefringence) exhibits two contributions, which can be associated respectively with the direct dispersive effect of dye molecules (terms with η_g' and η_e') and the effect of host molecules (terms with η_h'). The former is due both to the overall anisotropy induced in the dye population if $D_e \neq D_g$ and to the difference in polarizability of dye molecules in the ground and excited states if $\eta_e' \neq \eta_g'$. The host term is instead related only to the host orientation, driven by the optical field via the direct coupling with molecule polarization and by the additional photoinduced dye molecule field. The host term is expected to dominate the nonlinear birefringence in all materials where collective orientational effects are sufficiently strong. In particular, its effect is larger when the temperature factor $T^*/(T-T^*)$ is increased by lowering the temperature and it tends to diverge for $T \to T^*$. Such enhancement can indeed be observed for *liquid crystals in their isotropic phase* when approaching the transition to nematic phase [11]. However, this pretransitional divergence is truncated because the actual transition temperature T_c is always slightly larger than T^*. In liquids that do not exhibit a nematic phase, the constant T^* is usually well below the liquid-solid transition temperature and therefore a strong pretransitional enhancement cannot be observed. Note that the observation of this pretransitional temperature behavior is the signature of a collective orientational response (although not necessarily due to the dye field).

The ratio of the total host nonlinear birefringence to the sole ordinary Kerr contribution is the dye-induced enhancement of optical nonlinearity

$$A(I) = 1 + \frac{\Delta u Q_e}{(\eta_h N_t / nc) I} = 1 + \frac{2n\alpha_0 \lambda \tau_d \Delta u}{5 \eta_h N_t h} f(I). \qquad (28)$$

In particular $A(0)$ is the enhancement factor for $I \ll I_s$. To estimate it, we need to determine the value of η_h. We may consider the case of a nematic liquid crystal, for which the optical dielectric anisotropy is $\epsilon_a \approx \eta_h N_t S$, where S is the order parameter. As typically $\epsilon_a \approx S$, we obtain $\eta_h N_t \approx 1$. A more precise estimate should take into account also the variation of density and local-field factors when passing from the isotropic to the nematic phase. Taking $\tau_d \approx 1$ ns and $\Delta u \approx 0.1$ eV, we get $A(0) \approx 1 + 10^4 (\lambda \alpha_0)$. For $\lambda = 0.5$ μm and $\alpha_0 = 20$ cm^{-1}, we obtain $A(0) \approx 10$.

Let us now consider the case of a pure absorbing liquid. The steady-state solution in this case is

$$N_e = \frac{\alpha_0 \tau_e}{h \nu} I,$$

$$Q_e = \frac{2 \alpha_0 \tau_d}{5 h \nu} I, \tag{29}$$

$$Q_g = \frac{T^*}{u_{gg}(T - T^*)} \left(\frac{\eta_g N_t}{nc} I + u_{qe} Q_e \right) - \frac{D_e T}{D_g (T - T^*)} Q_e.$$

The nonlinear dielectric anisotropy is then

$$\Delta \epsilon = \eta'_e Q_e + \eta'_g Q_g = \left(\eta'_e - \frac{D_e}{D_g} \eta'_g \right) Q_e$$

$$+ \frac{\eta'_g T^*}{u_{gg}(T - T)^*} \left(\frac{\eta_g N_t}{nc} I + \Delta u Q_e \right), \tag{30}$$

with

$$\Delta u = u_{ge} - \frac{D_e}{D_g} u_{gg}. \tag{31}$$

Note the similarity between these results for the nonlinear birefringence and the dye-doped case. Indeed, the latter reduces to the former for $I \ll I_s$ [so that $f(I) = 1$] and with the substitution of the subscript h with g. In the pure material case one cannot distinguish the contributions of the ground-state dye and host. However, one still has separate individual and collective contributions having the same physical meaning as in the case of dye-doped materials. The saturation behavior, not investigated here, is instead expected to be different in the pure material case because the condition $N_d \ll N_t$ does not hold (on the contrary, $N_d = N_t$).

III. EXPERIMENT

We now discuss the predictions of the model in comparison with the results of our experiment.

A. Measurement of nonlinear birefringence

The material employed in our experiment was obtained by dissolving a small amount of dye in a transparent liquid host. The dye was the 1,8-dihydroxy 4,5-diamino 2,7-diisopentyl anthraquinone, an anthraquinone derivative that has good stability and is not liable to photoinduced conformational or chemical transformations in the visible domain. The host was the isotropic phase of the commercial liquid crystal mixture
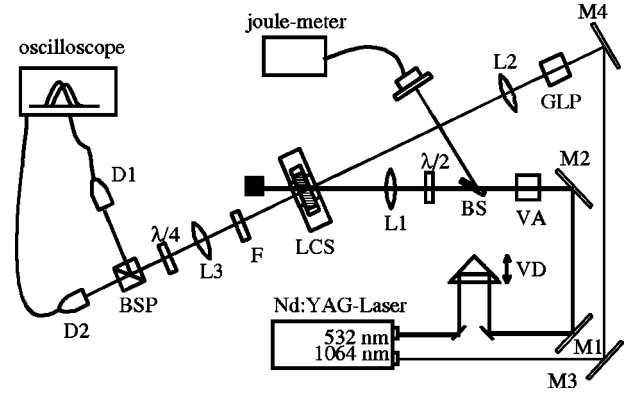

FIG. 2. Experimental setup. Legend: M, mirror; L, lens; F, filter; BS, beam splitter; BSP, beam-splitter polarizer; GLP, Glan laser polarizer; D, detector; VA, variable attenuator; $\lambda/2$, half-wave plate; $\lambda/4$, quarter-wave plate; LCS, liquid-crystal sample; VD, variable delay arm.

E63 by Merck, whose components are listed in Ref. [12]. The dye concentration was of 0.26% by weight. This specific mixture was chosen because it shows a large absorption-induced enhancement of the optical nonlinearity in the nematic phase [5]. At the pump wavelength $\lambda = 532$ nm, this mixture has $\alpha_0 = 22$ cm^{-1}. The sample was made by sandwiching a liquid film of thickness $L = 600$ μm between two plane glass substrates. Another sample of pure E63 was used as a reference. During the experiment, the sample was placed in a oven for temperature control within 0.1 K.

To measure the nonlinear birefringence, we used the pump and probe experimental geometry shown in Fig. 2. The pump beam was generated by a frequency-doubled Nd:YAG laser (where YAG denotes yttrium aluminum garnet), having $\lambda = 532$ nm, within the absorption band of the dye, and it was focused on the sample in a spot having a $1/e^2$ radius $w_0 = 270$ μm. The pulse duration (full width at half maximum) was $\tau_p = 22$ ns and the repetition rate was 10 Hz. For probing we used the fundamental radiation of the Nd:YAG laser at $\lambda' = 1064$ nm, outside the absorption band, to minimize the direct contribution of dye molecule to the nonlinear birefringence.

The polarization plane of the probe beam at the input of the sample formed an angle of 45° with that of the pump. As a result of the birefringence induced by the pump, the polarization of the probe becomes elliptical after passing through the sample. Its ellipticity is given by the Stokes parameter $s_3 = (I_+ - I_-)/(I_+ + I_-)$, where I_+ and I_- are the right and left circular polarization intensity components. To measure I_+ and I_- and thus determine s_3, we used a $\lambda/4$ plate, a polarizing beam splitter, and the detectors $D1$ and $D2$, as shown in Fig. 2. A small phase shift ϕ between ordinary and extraordinary waves results in $s_3 = \sin\phi \approx \phi$.

However, unless the probe spot size w_1 is much smaller than the pump one w_0, the transverse spatial dependence of the phase shift cannot be ignored. The transverse profile of the pump intensity $I(r)$ is reflected in a similar bell-shaped profile $\phi(r)$ of the phase shift. What we actually measured was the total power $P_\pm = \int I_\pm dA$ of each circular component of the probe, where the integration is over the cross section of the beam. The recorded signal was then obtained as
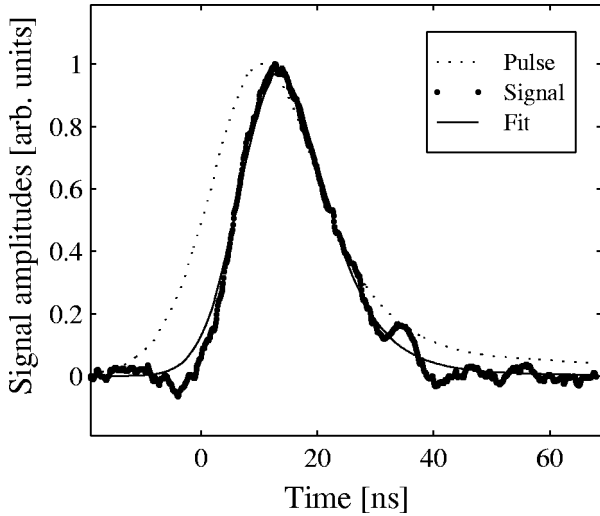
FIG. 3. Time behavior of the signal difference $P_+ - P_-$ of the readings of the two fast detectors $D1$ and $D2$. The dotted line is the pump pulse. The solid line is a fit to the signal, as described in the text.

$$\bar{s}_3 = \frac{P_+ - P_-}{P_+ + P_-} \simeq \frac{\int \phi(r) I_{\text{probe}} dA}{\int I_{\text{probe}} dA}. \tag{32}$$

In other words, our signal corresponds to the average phase shift experienced by the probe beam, weighted with the probe intensity profile. In our case, the probe diameter was somewhat larger than the pump one, for practical reasons. Then the approximate result $\bar{s}_3 \simeq K\phi(0)$ holds for sufficiently small pump intensity, with $K \simeq w_0^2/(w_0^2 + w_1^2)$. For larger pump intensities, when the phase shift saturates, this simple result is modified. Other factors can also contribute to complicate the above result or to modify the expression of K as, for example, the fraction of probe light effectively detected (light-diffusing plates were placed before the detectors to minimize the sensitivity to setup misalignments and light diffraction) and the diffraction induced in the probe beam by the phase-shift transverse profile. For this reason, we preferred not to perform absolute measurements of ϕ, but rather to refer all measurements to the transparent sample.

The phase-shift signal was detected by fast photodiodes ($D1$ and $D2$), so that its time behavior could be followed. The pump-probe pulse delay was adjusted to zero. An example of the recorded pump and signal pulses is shown in Fig. 3, referred to the same origin of time. A delay of several nanoseconds of the signal rise with respect to the pump is evident. This delay was observed in both the absorbing and transparent samples. Therefore, we ascribed it essentially to the finite orientational response time τ_h of the liquid, as discussed in detail later.

B. Secondary effects of light absorption

For a correct comparison of the nonlinearities $\Delta n(I)$ of the absorbing and transparent samples, it is necessary to take into account two secondary effects of absorption: light inten-

sity reduction and local temperature increase. The probe phase shift ϕ is related to the birefringence Δn by the equation

$$\phi = (2\pi/\lambda') \int_0^L \Delta n(z) dz, \tag{33}$$

where z is a coordinate along the probe propagation direction. In transparent samples Δn is independent of z and we obtain the simple proportionality $\phi(I) = (2\pi L/\lambda')\Delta n(I)$. In absorbing samples, however, the light intensity I and therefore the nonlinear birefringence $\Delta n(I)$ are functions of z because of absorption losses. In particular, for small intensities, we have $\Delta n(z) \propto I(z) = I_0 \exp(-\alpha_0 z)$. For higher intensities, when dye bleaching effects are important, both functions $I(z)$ and $\Delta n(z)$ must be determined numerically for every given input intensity I_0. In this way, we calculated the nonlinear loss factor $r_1(I_0)$ such that $\phi(I_0) = r_1(I_0)(2\pi L/\lambda')\Delta n(I_0)$ in the absorbing sample. In the limit of small light intensity, this factor is reduced to the standard expression $r_1 = [1 - \exp(-\alpha_0 L)]/\alpha_0 L$.

Light-absorption-induced heating has two effects that must be taken into account. First, it may directly modify the refractive index, so that there is a thermal optical nonlinearity (thermal lensing) that must not be confused with the photoinduced nonlinearity. This should not occur in principle because we measure only the anisotropic nonlinearity, i.e., the nonlinear birefringence, which is unaffected by the isotropic thermal lensing. However small misalignments in the setup could give rise to a spurious signal. To distinguish the anisotropic signal from this spurious isotropic contribution, for each data point we switched the pump polarization plane from 45° to −45° with respect to the probe polarization plane. The anisotropic contribution is then sign inverted while the spurious one is unchanged. By this method we found that the spurious contribution was actually less than 20% of the anisotropic signal. To cancel it almost completely, we then took the difference between the two signals.

The second effect of heating is the modification of all constants that depend on temperature and that enter Eq. (27) for $\Delta\epsilon$. In particular, in our case, the most sensitive to heating is clearly the factor $(T - T^*)^{-1}$. A local temperature increase by ΔT is therefore expected to reduce the nonlinearity of the absorbing sample approximately by a factor $r_2(I_0) = (T - T^*)/[T - T^* + \Delta T(I_0)]$, where T is the sample background temperature.

To take into account this effect, we performed a numerical simulation of the process of heat generation and diffusion. An example is shown in Fig. 4. After each pulse, the local temperature within the illuminated region is instantaneously (i.e., during the pulse passage) raised by $\Delta T_p \approx 3.5$ K/mJ of incident energy (at the birefringence peak $\Delta T_p \approx 2$ K/mJ). This corresponds to the expression $\Delta T_p = \Delta E_a/\rho V c_p$, where ΔE_a is the light energy absorbed in the liquid volume V, ρ is density, and c_p is the specific heat capacity at constant pressure. Next, the heat diffuses away, but the temperature does not relax completely before the next pulse arrives. Therefore, there is also a cumulative effect that, after a few pulses, stabilizes to an average increase of $\Delta T_c \approx 3$ K/mJ of single-pulse incident energy.
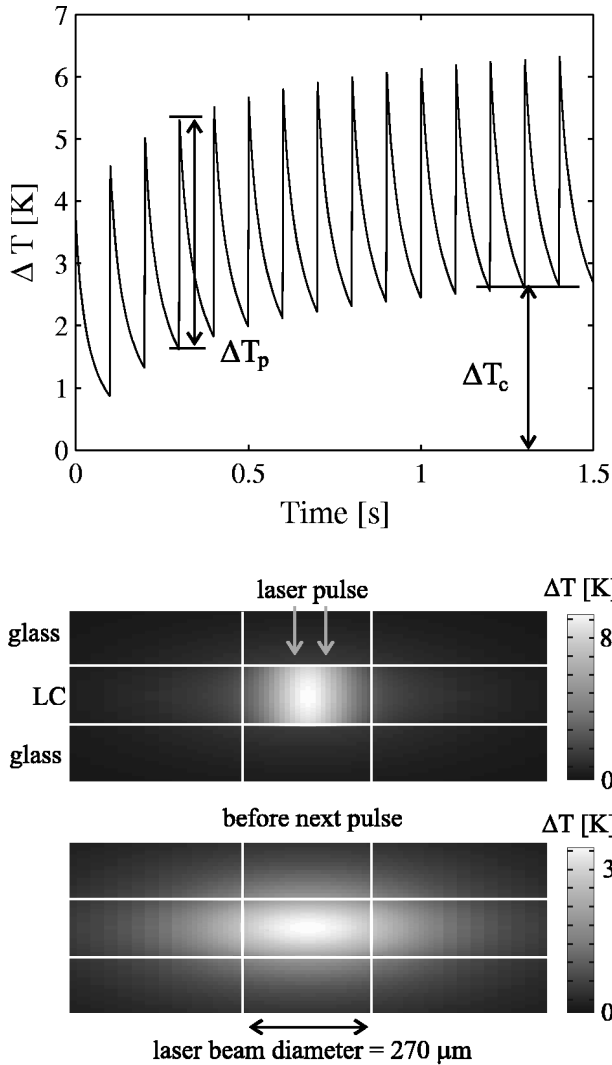
FIG. 4. Results of simulations of laser-induced heating in the sample for a pulse energy of 1 mJ: top, time behavior of temperature increase averaged over the sample illuminated volume; bottom, spatial distribution of thermal effects just after a laser pulse and just before the next one.

However, we must take into account still another effect: The birefringence is probed at a time that is within 10 ns after the peak of the absorbed pulse. In such a time, the liquid density cannot follow the temperature increase, as the sound wave front travels away from the beam in a time of order $\tau_s = w_0/v_s \sim 200$ ns, where $v_s \sim 1500$ m/s is the sound speed. Therefore, the heating initially occurs at constant volume rather than pressure. This has two important consequences: First, the immediate temperature increase to be considered is $\Delta T_p' = (c_p/c_v)\Delta T_p$, where c_v is the heat capacity at constant volume; second, the effects of a large pressure increase $\Delta p = (\partial p/\partial T)_V \Delta T_p'$ must also be taken into account. From $\Delta p \approx 3\rho v_s^2 \alpha \Delta T_p'$, where $\alpha = 1/3V(\partial V/\partial T)_p$ is the thermal linear expansion coefficient, we estimate $\Delta p/\Delta T_p' \approx 3$ MPa/K. For our purposes, the most important effect of this pressure increase is the shifting of the isotropic-nematic transition point T_c and therefore of T^*. A typical value is $dT_c/dp \approx 0.3$ K/MPa. Therefore, $\Delta T^* \approx \Delta T_p'$ and the factor $(T-T^*)^{-1}$ is only weakly affected by the instan-

taneous heating. This almost complete compensation can be explained if the free-energy coefficient u_{hh} controlling T^* is mainly of entropic nature (for example, due to excluded volume effects). In such a case, indeed, *at constant density* we would have $T^* \propto u_{hh} \propto T$ and the factor $T^*/(T-T^*)$ would be approximately independent of temperature T. In view of this analysis, we neglected the contribution of instantaneous heating and calculated the factor r_2 including only the effect of cumulative heating ΔT_c.

In conclusion, the phase shift signal measured in the absorbing sample was related to the birefringence by the expression

$$\phi(I_0) = r_1(I_0)r_2(I_0)\frac{2\pi L}{\lambda'}\Delta n(I_0). \qquad (34)$$

Actually, in our case the factor $r_1(I_0)r_2(I_0)$ turns out to be weakly dependent on the pump energy, so $r_1 r_2 \approx 0.6$ almost independently of I_0. The nonlinearity enhancement ratio was calculated from the measured phase shifts as

$$A(I_0) = \frac{\Delta n_{\text{abs}}}{\Delta n_{\text{transp}}} = \frac{1}{r_1(I_0)r_2(I_0)}\frac{\phi_{\text{abs}}(I_0)}{\phi_{\text{transp}}(I_0)}. \qquad (35)$$

C. Experimental results

An anisotropic phase-shift signal was observed both with the dye-doped sample and with the reference pure sample. In all cases the signal in the former was significantly larger than in the latter, but for other features they were rather similar. A typical phase-shift signal is shown in Fig. 3. We investigated the dependence of the phase-shift signal peak in the dye-doped sample and in the pure reference sample on pump pulse energy at fixed background temperature and on temperature at fixed pump energy. Moreover, we studied the response time τ_h of the signal at varying temperatures. Although τ_h was several nanoseconds, we assumed that the pump pulse was long enough that the signal peak approximated well a steady-state condition. Therefore, we compared the signal peak with the theoretical predictions of Sec. II C.

Let us consider the energy dependence first. The phase-shift data versus energy measured with the pure sample are shown in Fig. 5 as squares. In the investigated range of pump energies no saturation of the orientational response can occur, as the pump peak intensity $I \sim 10^7$ W/cm^2 is five orders of magnitude smaller than I_K. The data were therefore fitted by a straight line. Actually, in Fig. 5, both data and line are inversely corrected for the factor $(r_1 r_2)^{-1}$, in order to compare them with the results in the dye-doped sample (which we preferred to leave unaltered, as they are our main results).

The phase-shift data for the dye-doped sample are shown in Fig. 5 as circles. In this case a saturation behavior is evident, which must be related to dye bleaching, as light peak intensities are of the order of I_s. Figure 6 shows the nonlinearity enhancement A versus energy calculated from these data using Eq. (35). The line in Fig. 6 is our theoretical prediction based on Eq. (28) or, equivalently, $A(I) = 1 + [A(0)-1]f(I)$, with $f(I)$ given by Eq. (26). The constant $A(0)$ was adjusted for the best fit, obtaining $A(0) = 21 \pm 4$. We note, however, that $A(0)$ can be obtained also without any reference to a definite model, by direct extrapolation of
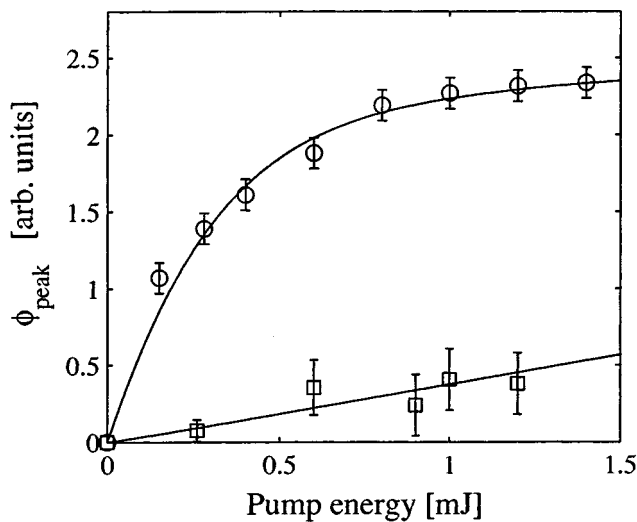
FIG. 5. Measured phase shift (peak values) versus pump pulse energy in the transparent pure liquid (squares) and in the dye-doped absorbing liquid (circles). The lines are our theoretical predictions.

FIG. 7. Difference between the phase shift measured in the dye-doped sample and the corresponding one in the transparent sample versus the pump pulse energy, providing the contribution to the optical nonlinearity of the photoinduced molecular field only. The line is our theoretical prediction.

the enhancement data to a vanishing pump energy, although this procedure leads to a greater uncertainty. The line shown in Fig. 5 is from Eq. (27) corrected for laser-induced heating and absorption losses, with $Q_e(I)$ as given in Eq. (24) [the direct effect of dye, i.e., the first term in Eq. (27), was neglected]. The unknown constants in Eq. (27) were referred to $A(0)$ and to the pure-sample signal, so that no further adjustment was needed in this case.

In Fig. 7 we plotted the points obtained as the difference between the dye-doped data and the corresponding pure-sample (corrected) data. These points show the contribution to molecular orientation of the photoinduced intermolecular-force field U_h^i only. The line is the prediction of our model. Considering that there is only one adjustable parameter in the theory, the agreement with the experiment is certainly satisfactory.

In evaluating the theory predictions, the values of τ_e and D_e were taken from Ref. [8], where they are obtained from
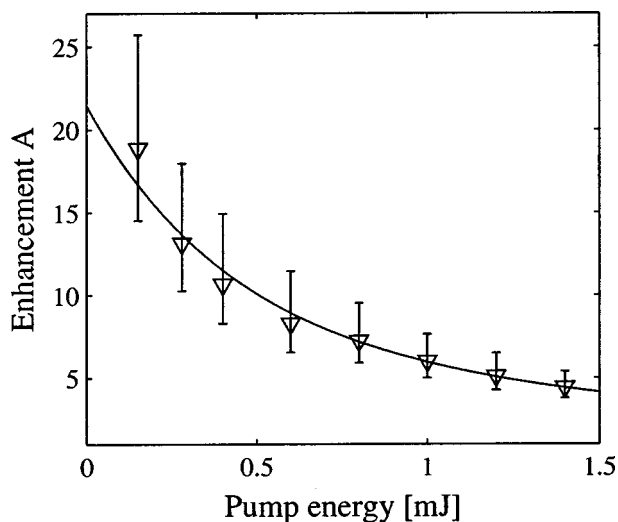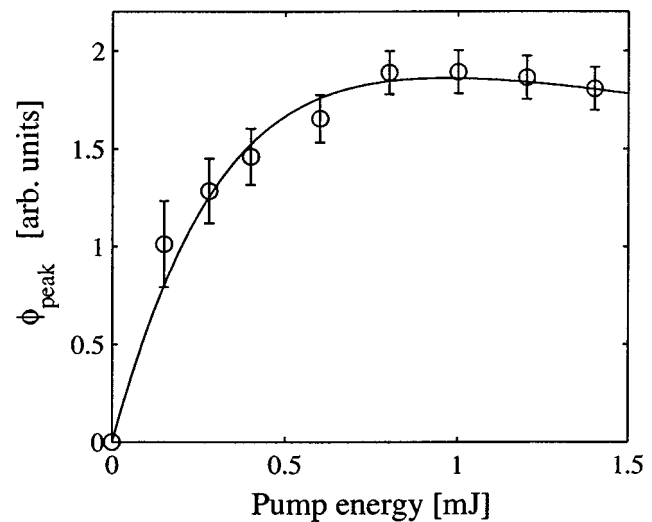

FIG. 6. Measured optical nonlinearity enhancement A due to the dye effect versus pump pulse energy. The line is a best fit of theory on the data, as described in the text.

measurements of time-resolved fluorescence. The pump energy scale of the theoretical curves was determined *a priori* from the peak intensity I, using the experimental values of the beam waist w_0 and pulse duration τ_p. To calculate $f(I)$ we had to make an assumption about the ratio D_g/D_e. First we assumed $D_e = D_g$. This already led to good agreement between theory and data, but for the best agreement the energy scale had to be finely adjusted by approximately 30%. Assuming instead $D_g/D_e \simeq 2$, this energy-scale adjustment is not necessary. However, this result cannot be considered a reliable estimate of D_g/D_e, as small discrepancies in the energy scale can be easily ascribed to several experimental nonidealities (ranging from the imperfect Gaussian shape of the spatial or temporal profile of the pump pulse to effects related to the transverse profile of the probe beam).

Let us now discuss the temperature behavior. The inverse peak signal measured at a given pump pulse energy and for varying temperature is shown in Fig. 8. The straight lines are from the linear best fit. Similar results are obtained for different pump pulse energies. The pretransitional $(T - T^*)^{-1}$ power law expected for an orientational optical nonlinearity is well reproduced in both the absorbing and transparent sample. We obtain $T^* = 78 \,°C$ in the transparent sample. In the absorbing sample, the apparent value of T^* is shifted by laser-induced heating (the data here are not corrected for heating) and therefore is pulse-energy dependent. We observe a decrease of about 5 K/mJ, in reasonable agreement with the results of our laser-induced heating calculations.

We also analyzed the time behavior of the signal in more detail in order to extract information on the material response time as a function of temperature. We assumed that the phase shift $\phi(t)$ of the material follows a standard relaxation law of the form $\tau\dot\phi + \phi = kI(t)$, where $I(t)$ is the pump pulse time profile and τ is the response time. This relaxation law can be numerically integrated with the experimental pulse profile $I(t)$ as the driving term. We used these numerical solutions to fit the measured phase-shift pulse by adjusting the time constant τ. Our results for the case of the dye-doped
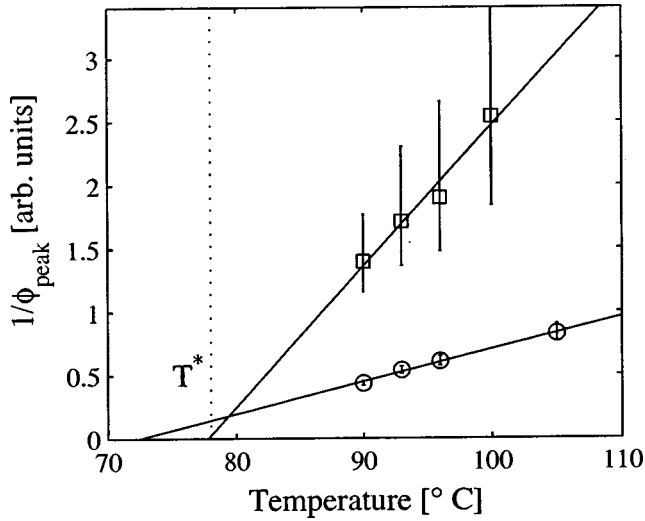
FIG. 8. Inverse phase-shift signal versus sample temperature for a pump pulse energy of 1 mJ in the pure sample (squares) and in the dye-doped sample (circles). The lines are from the linear best fit. T^* is the critical temperature for instability of the isotropic phase (a few degrees lower than the transition point T_c).

sample are shown in Fig. 9 for a given pump energy. Similar results were obtained at different pump energies and with the transparent sample (although in the latter the data are very noisy as the signal was smaller). Again we find a pretransitional behavior in good agreement with the power law $\tau \propto (T - T^*)^{-1}$, where T^* is consistent with the value obtained from the birefringence pretransitional behavior. It is then natural to identify τ with the host orientational response time τ_h, which is predicted to exhibit a pretransitional behavior according to Eq. (19). Our results are also in good agreement with independent measurements of τ_h based on the pump and probe optical Kerr effect in pure E63 with picosecond pulses [13].

IV. DISCUSSION

We developed a model of the molecular orientation induced in an absorbing liquid made of elongated molecules.
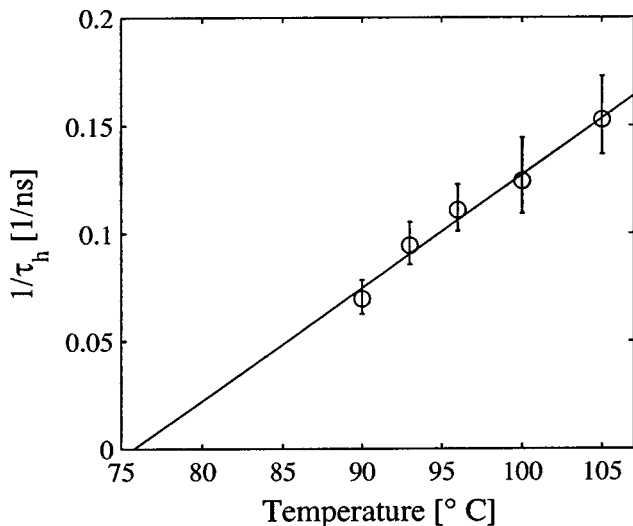

FIG. 9. Inverse orientational response time τ_h versus temperature, as measured for a pump pulse energy of 0.6 mJ. The line is from the linear best fit.

The model is based on the assumption that a photoexcited molecule interacts with its neighbor molecules differently from the ground-state molecules. This results in an enhancement of the optical Kerr effect of a transparent liquid when it is doped with a small amount of dye. Such a prediction has been verified in our experiment of pump-and-probe nonlinear birefringence. For our choice of materials, the observed enhancement is of about one order of magnitude for dye concentrations of 0.1%, but we cannot exclude the possibility of having even larger enhancements for different materials. The model correctly predicts also the saturation behavior of the birefringence for increasing pump pulse energy and the temperature dependence of the signal peak and rise time.

In the presence of light absorption one has to be very careful when interpreting the optical nonlinear response because thermal and dye saturation effects can be strong. We modeled both these effects in order to estimate their contribution. We made sure that the nonlinearity we observed was indeed anisotropic, i.e., it corresponded to a light-induced birefringence and therefore could not be ascribed to heating or other isotropic effects. Moreover, we verified that the principal axes of the induced birefringence were dictated by the optical electric field, thus excluding effects related to flow, gradients, or any other anisotropic effects unrelated to the light field. The direct dye contribution to nonlinearity, which can also be anisotropic, was minimized by adopting a probe wavelength outside the absorption band of the dye. However, the strongest evidence that the birefringence was indeed due to photoinduced molecule reorientation is provided by the pretransitional effects observed when the temperature of our material approached the transition point from the isotropic liquid phase to the nematic liquid-crystal phase. These effects were observed both in the signal amplitude and in the response time.

The only unknown molecular quantity contained in our model is the energy constant $\Delta u = u_{he} - u_{hg} D_e / D_g$, which quantifies the variation of intermolecular interactions between the dye and host occurring when the dye is photoexcited and determines the magnitude of the nonlinearity enhancement $A(0)$. From the measured value of $A(0) = 21 \pm 4$ we obtain $\Delta u = 0.18 \pm 0.05$ eV [14].

Let us now analyze this result in more detail. In Ref. [16], the value of u_{hg} was estimated from the measured dichroism when the mixture is in its nematic liquid-crystal phase, obtaining $u_{hg} \approx 0.6$ eV. If we assume $D_g = D_e$, we then obtain $u_{he} \approx 0.8$ eV, i.e., an increase by 30% in the orientational energy. If we assume instead $u_{he} = u_{hg}$ we obtain $D_g / D_e \approx 1.4$. These results are not unreasonable, although they imply significant variations of molecular properties as a consequence of electronic excitation.

However, measurements performed in the nematic phase on the same mixture used in our experiment have shown that the ''constant'' quantity $\Delta u \tau_d$ controlling the enhancement factor A actually depends on the pump wavelength λ [16,17]. This unexpected behavior could be explained by the presence of more than one excited level [16]. The wavelength for which the enhancement is maximum in the nematic phase is $\lambda = 630$ nm. If we apply to the isotropic phase the same wavelength dependence observed in the nematic phase, we obtain $\Delta u \approx 0.3$ eV for $\lambda = 630$ nm (τ_d was determined from Ref. [8]). This corresponds either to $u_{he} / u_{hg} = 1.5$ if D_e

$=D_g$, or to $D_g/D_e \approx 2.1$ if $u_{he} = u_{hg}$. Of course also intermediate cases are possible with the contributions to Δu coming from both changes. These estimates may appear not very plausible, as the relative variations are quite large. However, there are theoretical reasons supporting the possibility of large changes in the rotational diffusion constant, as discussed in Ref. [16]. Moreover, the preliminary results of an experiment of nonlinear dichroism currently under way also seem to imply a ratio D_g/D_e greater than 2 [18]. If these surprising results are confirmed, we may say that the phenomenon of photoinduced molecular orientation in absorbing liquids will be substantially understood.

[1] Y. R. Shen, *The Principles of Nonlinear Optics* (Wiley, New York, 1984), p. 291.

[2] R. W. Boyd, *Nonlinear Optics* (Academic, Boston, 1992), p. 178.

[3] D. Paparo, L. Marrucci, G. Abbate, E. Santamato, M. Kreuzer, P. Lehnert, and T. Vogeler, Phys. Rev. Lett. **78**, 38 (1997).

[4] R. Muenster, M. Jarasch, X. Zhuang, and Y. R. Shen, Phys. Rev. Lett. **78**, 42 (1997).

[5] I. Jánossy, A. D. Lloyd, and B. S. Wherret, Mol. Cryst. Liq. Cryst. **179**, 1 (1990).

[6] I. Jánossy, L. Csillag, and A. D. Lloyd, Phys. Rev. A **44**, 8410 (1991).

[7] I. Jánossy, Phys. Rev. E **49**, 2957 (1994).

[8] D. Paparo, L. Marrucci, G. Abbate, E. Santamato, P. Bartolini, and R. Torre, Mol. Cryst. Liq. Cryst. Sci. Technol., Sect. A **282**, 461 (1996).

[9] Actually this quadratic approximation is justified *a priori* only if the distributions f_α can be considered "small" in some sense. It can be shown that it suffices to require that the anisotropic fraction be small, i.e., $|f_\alpha - N_\alpha/4\pi| \ll N_t$. In our case this condition is verified by the dye population because its concentration N_d/N_t is small and by the host population because its anisotropy is small.

[10] S. Chandrasekhar, *Liquid Crystals*, 2nd ed. (Cambridge University Press, Cambridge, 1992), p. 62.

[11] G. K. L. Wong and Y. R. Shen, Phys. Rev. Lett. **30**, 895 (1973); Phys. Rev. A **10**, 1277 (1974).

[12] A. Jákli, D. R. Kim, M. R. Kuzma, and A. Saupe, Mol. Cryst. Liq. Cryst. **198**, 331 (1991).

[13] P. Bartolini, D. Paparo, and R. Torre (unpublished).

[14] We used the value $\eta_h N_t = 0.95 \pm 0.05$, determined from the birefringence of the nematic phase, as described in Sec. II. In this calculation we took into account also the changes of density and local-field factors with temperature. Actually, local-field effects in the nematic phase are still a matter of debate [15]. Our working assumption was that the same local-field factors determining the nematic birefringence apply to the nonlinear birefringence in the isotropic phase, except for the small temperature dependence. Note, moreover, that the quoted value of Δu is slightly different from that of Ref. [3]. The latter was actually incorrect because of a mistake in our calculations.

[15] J. Kędzierski, Z. Raszewski, J. Rutkowska, W. Piecek, P. Perkowski, J. Zmija, R. Dąbrowski, and J. W. Baran, Mol. Cryst. Liq. Cryst. Sci. Technol., Sect. A **282**, 205 (1996).

[16] L. Marrucci, D. Paparo, P. Maddalena, E. Massera, E. Prudnikova, and E. Santamato, J. Chem. Phys. **107**, 9783 (1997).

[17] D. Paparo, P. Maddalena, G. Abbate, E. Santamato, and I. Jánossy, Mol. Cryst. Liq. Cryst. Sci. Technol., Sect. A **251**, 73 (1994).

[18] M. Kreuzer, D. Paparo, and L. Marrucci (unpublished).